Author Manuscript

Title: Lewis Acid-Tethered (cAAC)–Copper Complexes: Reactivity for Hydride Transfer and Catalytic CO2 Hydrogenation

Authors: Hayoung Song, PhD; Nathaniel Kolnik Szymczak, Ph.D.

This is the author manuscript accepted for publication. It has not been through the copyediting, typesetting, pagination and proofreading process, which may lead to differences between this version and the Version of Record.

To be cited as: 10.1002/ange.202411099

Link to VoR: https://doi.org/10.1002/ange.202411099

Lewis Acid-Tethered (cAAC)–Copper Complexes: Reactivity for Hydride Transfer and Catalytic CO_2 Hydrogenation

Hayoung Song and Nathaniel K. Szymczak *

Department of Chemistry, University of Michigan, Ann Arbor, Michigan 48109, United States

Supporting information for this article is given via a link at the end of the document

Abstract: We present a series of borane-tethered cyclic (alkyl)(amino)carbene (cAAC)-copper complexes, including a borane-capped Cu(I) hydride. This hydride is unusually hydridic and reacts rapidly with both CO_2 and 2,6-dimethylphenol at room temperature. Its reactivity is distinct from variants without a tethered borane, and the underlying principles governing the enhanced hydricity were evaluated experimentally and theoretically. These stoichiometric results were extended to catalytic CO_2 hydrogenation, and the borane-tethered (intramolecular) system exhibits ~3-fold enhancement relative to an intermolecular system.

Copper hydrides are widely implicated as catalytic intermediates for challenging small molecule reductions and regio- and enantioselective hydrofunctionalization reactions.[1] To promote these reactions, extensive effort has focused on strategies to generate highly reactive copper hydrides. In contrast to Stryker's reagent,[2] a high-nuclearity Cu–H cluster, low coordinate Cu–H compounds are typically much more reactive[3] and can be prepared using sterically encumbered N-heterocyclic carbenes (NHCs).[4] Although often prepared using hydride donors,[4a-e,5],[6] the generation of copper hydrides using H_2 is an attractive, yet underdeveloped strategy.[7] Select examples illustrate the feasibility of this approach through either hydrogenolysis of copper alkoxides[8],[9], or alternatively, by addition of a Lewis acid and base to promote H_2 heterolysis via a Frustrated Lewis Pair (FLP).[10]

Lewis acids can influence and potentially enhance Cu–H based reactivity in one of two ways, by: 1) generating hydrides from H_2 through FLP-type pathways,[11] and 2) increasing stability of the otherwise highly reactive Cu–H intermediates.[4f,9b,12] These enhancements can enable catalytic applications of borane-stabilized cuprous hydrides under conditions that would otherwise be incompatible (e.g. aqueous solutions[12a,12c]). For example, the Bertrand group recently reported that mixtures of 1,8-diazabicyclo(5.4.0)undec-7-ene (DBU) and $B(C_6F_5)_3$ are capable of activating H_2 at elevated temperature and pressure.[11a] This system is proposed to operate through a FLP-type mechanism, wherein the borane and DBU heterolytically cleave H_2 to form [HDBU][HB(C_6F_5)$_3$] that reacts with a cyclic (alkyl)(amino)carbene (cAAC)-copper complex. The resulting masked cuprous hydride (^{Et}cAAC)CuH(B(C_6F_5)$_3$) is active for catalytic CO_2 hydrogenation (TON = 305 – 1881, **Figure 1**, top). In related work highlighting improved stability, the Cantat group reported that a BEt_3 additive enabled access to a monomeric masked cuprous hydride.[9b] In addition to these advantages, an important consideration for Lewis acid additives in copper hydride chemistry is their potential to engage in unproductive acid/base reactions, which can attenuate reactivity of the hydride or alternatively, inhibit product release. For example, although a strong Lewis acid facilitates FLP activation of H_2 in Bertrand's report, the resulting Cu–H–B(C_6F_5)$_3$ is *deactivated* toward hydride transfer to CO_2 (**Figure 1**, top).[11]

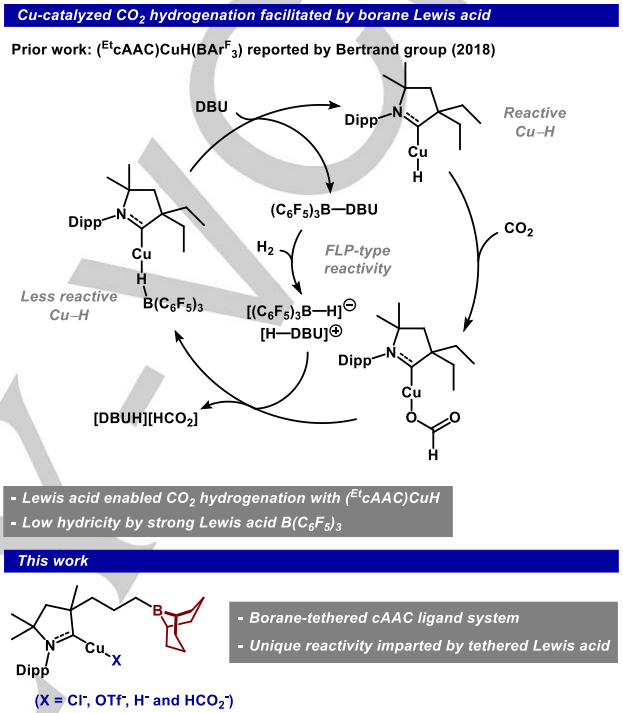


Figure 1. Top: FLP mediated CO_2 hydrogenation using a cAAC–Cu complex and proposed mechanism. Bottom: design strategy to incorporate a tethered borane within a cAAC–Cu complex (Dipp = 2,6-diisopropylphenyl).

Efficient CO_2 hydrogenation catalysts are often correlated with strong hydricity of the metal hydride.[13] Unfortunately, introduction of strong Lewis acids to M–H species (e.g. M–H–BR_3) generally decreases their hydricity.[11a] This challenge can potentially be attenuated by using weaker Lewis acids: decreasing the M–H–BR_3 interaction energy may facilitate access to catalytically active M–H species. In spite of these desirable attributes, moderate strength Lewis acid-masked cuprous hydrides are generally thermally unstable, and trialkylborane-capped (cAAC)CuH are inaccessible, which prevents their isolation.[4b,12b]

One general strategy for accessing cuprous hydrides capped by moderate-strength Lewis acids is to develop monodentate carbene ligands such as cAACs that contain appended Lewis acids (**Figure 1**, bottom). This approach allows weaker strength Lewis acids to be used: a consequence of kinetically favorable binding imparted by an intramolecular system. Although incorporating appended Lewis acidic boranes into ligand frameworks is a growing strategy to enable unique reactivity,[12d,14] intramolecular acid/base quenching is an unproductive competitive pathway, and there are no examples of monodentate carbenes that contain appended Lewis acids, such as 9-BBN (acceptor number, AN = 24.9),[14f] that are more acidic than BPin (AN = 10.0).[15] In this manuscript, we develop a Lewis acid-tethered cAAC ligand that enables access to a highly reactive masked cuprous hydride and demonstrate its competence for hydride transfer within the context of catalytic CO_2 hydrogenation.

Author Manuscript

This article is protected by copyright. All rights reserved

We targeted the preparation of borane-tethered cAAC complexes via hydroboration of an olefin-appended cAAC precursor.[16] Our previous study on the effect of borane tether length[14h] suggested that a three-carbon tether to the borane group was the most versatile for stabilizing metal-coordinated substrates. Therefore, we initially targeted a tether with three methylene units for the cAAC ligand (**Figure 2**). Treating a CH_2Cl_2 solution of [**1**]BF_4 with 2.45 equiv. 9-borabicyclo[3.3.1]nonane (9-BBN) for 12 h afforded [**2**]BF_4 in 70% yield. In contrast to many cAACs that can be isolated as a free carbene, deprotonation of [**2**]BF_4 using $KN(SiMe_3)_2$ did not afford a free carbene, and instead formed the intramolecular quenched Lewis acid/base adduct **3** in 68% yield. A single-crystal X-ray diffraction (SCXRD) study of **3** confirmed the connectivity, revealing an intramolecular cAAC/BBN Lewis pair structure. The B1–C1 bond length in the solid-state structure of compound **3** is 1.642(2) Å, similar to previously reported cAAC/boron Lewis pairs.[17] Solutions of **3** in C_6D_6 exhibited high stability in air (weeks) and under thermal conditions (70 ºC), highlighting the inertness of both the carbene and borane for subsequent reactivity. We found that the B–C bond remained intact even after refluxing a THF solution containing CuCl for 24 h. To overcome the acid/base incompatibility, we targeted late-stage hydroboration, a strategy previously employed for bi- and tridentate ligands.[14f,14j] The allyl-tethered cAAC–CuCl complex ((allylcAAC)CuCl, **4**) was prepared in one pot by introducing freshly thawed THF to 1 equiv. [**1**]BF_4, 1 equiv. CuCl and 1.05 equiv. $KN(SiMe_3)_2$. The ^{1}H- and ^{13}C-NMR spectra indicated metalation, as assessed by the disappearance of the C–H resonance (^{1}H: 9.29 ppm) and a downfield shift of the carbene resonance to 248 ppm in ^{13}C NMR spectrum. Importantly, the terminal olefin shifted minimally upon metalation (5.85 ppm and 5.21 ppm), consistent with no interaction with Cu. Introduction of 1.1 equiv. 9-BBN to a THF solution of **4** for 6 h afforded a new complex whose formation was monitored by ^{1}H NMR spectroscopy (disappearance of olefin resonances). The product, (BBNcAAC)CuCl (**5**), was obtained as colorless crystals by cooling a pentane-saturated solution. The solid-state structure of **5** was determined via SCXRD analysis, which indicated that the tethered borane group had no acid/base interactions (ΣB_α = 359.8 º). Metathesis of the chloride ligand with AgOTf was rapid and afforded (BBNcAAC)CuOTf (**6**), as assessed by NMR spectroscopy.

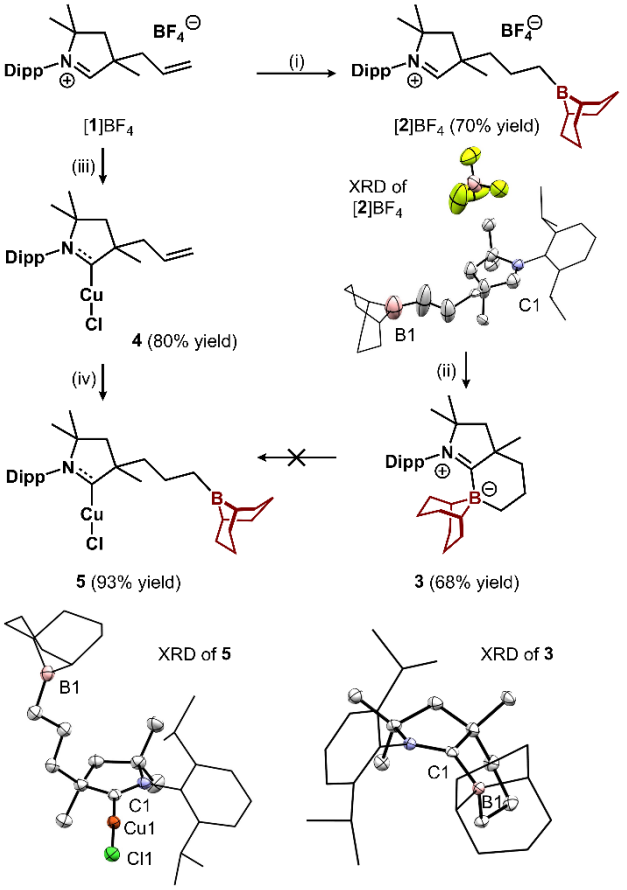


Figure 2. Synthesis of [**2**]BF_4, **3**, **4**, and **5**. (i) 9-BBN (2.45 equiv), CH_2Cl_2, rt, 12 h, (ii) $KN(SiMe_3)_2$ (1.05 equiv), THF, -108 ºC → rt, 1 h, (iii) CuCl (1.0 equiv), $KN(SiMe_3)_2$ (1.05 equiv), THF, -108 ºC → rt, 6 h, (iv) 9-BBN (1.1 equiv), THF, rt, 6 h, and solid-state structures of [**2**]BF_4, **3** and **5**.

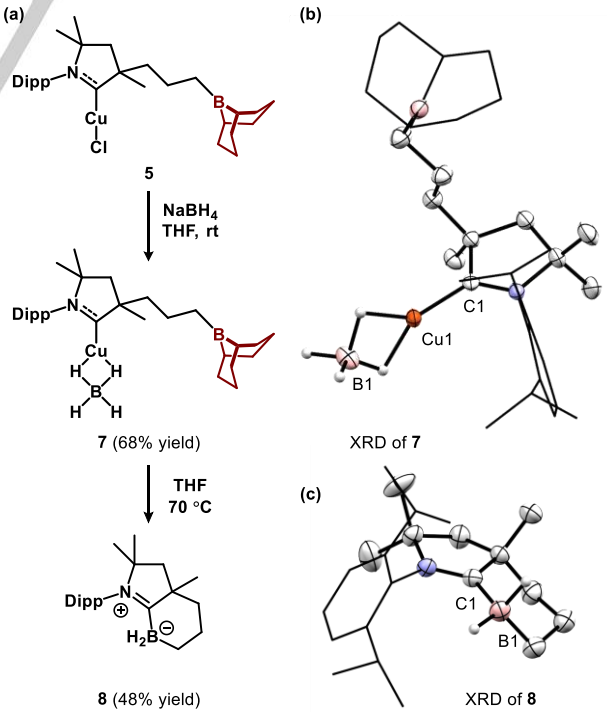


Figure 3. (a) Synthesis of **7** and **8**, (b) solid state structure of **7** and (c) **8**.

This article is protected by copyright. All rights reserved

Author Manuscript

We prepared a variant capable of reductive chemistry by introducing 5 equiv. of $NaBH_4$ to **5** in THF solvent at room temperature. This reaction afforded (^{BBN}cAAC)Cu-κ^2-BH_4 (**7**) (**Figure 3a**), wherein the borohydride ligand acts as a bidentate ligand (κ^2) to Cu. Note that analogous (cAAC)CuBH_4 complexes have been previously reported to act as precatalysts for CO_2 hydrogenation[11a] and ammonia-borane (BH_3NH_3) dehydrogenation.[12a] The ^{11}B NMR spectrum of **7** indicated two resonances (87.71 ppm; broad singlet, and -37.90 ppm; pentet, J_{B-H} = 84.2 Hz), consistent with a trigonal BBN environment and tetrahedral BH_4, respectively. A SCXRD study revealed identical bond distances for C1–Cu1 (1.892(2) Å) and Cu1–B1 (2.109(2) Å) when compared with previously reported (^{Et}cAAC)CuBH_4.[12a] Importantly, the structure confirmed the absence of any interactions between the appended BBN unit and the BH_4 unit (**Figure 3b**), a result that is consistent with literature reports; there are no structurally characterized compounds featuring a BH_4–BR_3 interaction.

Despite the absence of an interaction between the BH_4^- ligand and the appended BBN unit, we observed a thermally-induced chemical reaction between these groups, implicating the intermediacy of an adduct. For example, heating a THF solution of **7** to 70°C for 12 h afforded a new species containing a triplet at -24.28 ppm (J_{B-H} = 86.2 Hz) in addition to three broad singlet peaks in the ^{11}B NMR spectrum, corresponding to free 9-BBN (58.71, 29.21, and 15.13 ppm). SCXRD analysis revealed an intramolecular Lewis acid/base adduct **8** with no Cu.[18] Notably, the structure of **8** indicated a transborylation reaction between –BBN and $–BH_2$. This reaction type is precedented for catalytic hydroboration/transborylation,[19] and we propose it is facilitated in this case by the formation of a 6-membered heterocycle.

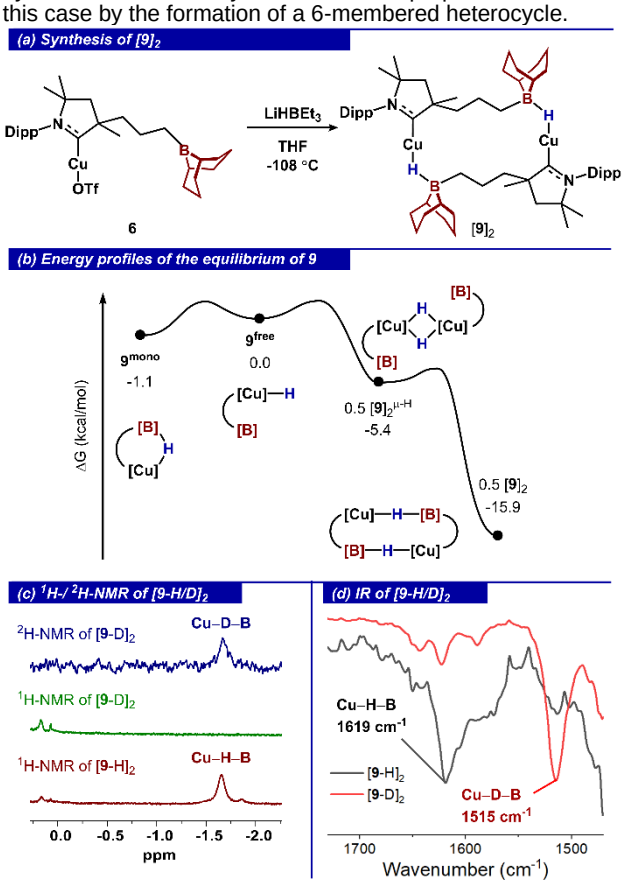


Figure 4. (a) Synthesis of [**9**]$_2$, (b) energy profiles of the equilibrium of **9** (Gibbs free energies were calculated by Gaussian 16 at *d3*-B3LYP/def2svp for Cu, 6-31+g(d,p) for B, C, N, H/CPCM(THF) level), (c) ^{1}H-/^{2}H-NMR of [**9**-H/D]$_2$ in THF, (d) Infrared spectrum (THF) of [**9**-H/D]$_2$ (Solvent peak is removed for clarity).

Based on the low thermal stability of **7**, we targeted an alternative route to generate (cAAC)Cu–H complexes that preserves the BBN-unit. In contrast to the thermal stability of triarylborane-masked (NHC)CuH (e.g. (IPr)CuH(BPh_3): 12 h at rt),[12c] trialkylborane (e.g. triethylborane; BEt_3)-masked analogs are considerably less stable (e.g. (6-sIPr)CuH(BEt_3): decomposes > -30 °C).[12b] Notably, the cAAC analog is not stable and dissociates BEt_3.[12b] Despite these observations using intermolecular Lewis acids, rapid addition of 1.2 equiv. Li$HBEt_3$ to **6** at -108 °C (10 minutes) (**Figure 4a**) afforded a new hydride complex (**9**), as assessed by ^{1}H-NMR spectroscopy. The high field region of ^{1}H-NMR spectrum revealed a broad singlet at -1.66 ppm in THF, consistent with related borane-masked cuprous hydrides (**Figure 4c**).[4f,9b,12b,12d] A deuterium labeling experiment using Li$DBEt_3$ caused the resonance at -1.66 ppm in the ^{1}H NMR spectrum to disappear, concomitant with the appearance of a new resonance in the ^{2}H-NMR spectrum at -1.65 ppm. IR analysis of **9** in THF revealed an absorption at 1619 cm^{-1} (**Figure 4d**), similar to previously reported (IPr)CuH(BPh_3) (1693 cm^{-1} in KBr).[12c] This absorption is sensitive to deuteride incorporation, undergoing a significant shift (ν_{Cu-D-B} = 1514 cm^{-1}) of 105 cm^{-1}. Collectively, these data are consistent with Cu–H–B character of **9**.

Although we confirmed the formulation of **9** *in situ*, we found that this compound was extremely sensitive to the presence of trace (<5 ppm) water, and attempts to obtain single crystals for X-ray diffraction experiments (pentane at -25 °C) afforded a hydroxo-bridged dimer **S13** (**Figure S47**). We propose that the inherent sensitivity prevented isolation of **9** in analytical purity (72% purity by quantitative ^{1}H-NMR spectroscopy). Notably, the structure revealed a preference for dimerization with a 1,1-binding *X*-type ligand. This result is similar to a previous report where a highly reactive copper hydride underwent hydrolysis during crystallization, precluding standard characterization.[4f]

To provide insight into the nature of the Cu–H environment in **9**, we performed a computational study to examine monomer/dimer speciation. The monomeric form (**9**^{mono}) exhibits an intramolecular Cu–H–B interaction that is slightly thermodynamically favorable compared to free Cu–H **9**^{free} (-1.1 kcal/mol, **Figure 4b**). However, dimerization of **9** *via* intermolecular Cu–H–B interactions is more thermodynamically favorable (-15.9 kcal/mol). In addition, another dimeric form, [(^{BBN}cAAC)Cu]$_2$(μ-H)$_2$ ([**9**]$_2^{\mu-H}$), is intermediate in stability between **9**^{mono} and [**9**]$_2$ (-5.4 kcal/mol). This result contrasts with the inaccessibility of a related monomeric (cAAC)Cu–H–BEt_3 complex.[12d] We attribute the higher stability of [**9**]$_2$ to the presence of the tethered borane, whose intramolecular Lewis acid enables H–B interactions with a low entropic penalty. In contrast, we propose that the lower stability of **9**^{mono} is due to ring strain imparted by the tethered BBN when binding to the linear (cAAC)Cu–H unit. This proposal is supported by a direct comparison between the stability of **9**^{mono} and (^{Et}cAAC)CuH with an exogenous (untethered) borane of similar Lewis acidity (EtBBN), which afforded a value of -7.4 kcal/mol (6.3 kcal/mol lower than **9**^{mono}, see SI). We used a DOSY (Diffusion Ordered Spectroscopy) experiment to examine the solution behavior of **9**. These experiments revealed a diffusion coefficient (*D*) of 1.22 × 10^{-9} m^2 for **9**, which is around half that of a well-defined reference monomer **5** (*D* = 2.13 × 10^{-9} m^2), and consistent with formulation of [**9**]$_2$ as a dimer. Thus, we propose that although solutions containing **9** exist primarily as a borane-capped dimeric complex [**9**]$_2$, equilibria with [**9**]$_2^{\mu-H}$ and **9**^{mono} may be kinetically accessible at room temperature, potentially providing a pathway to subsequent reactions.

Hydride transfer is one class of reactions that may be used to capitalize on the Cu–H adducts at either the monomer and/or dimer states. The hydricity of metal hydrides provides an important thermodynamic guideline that can be used to predict reactivity and ultimately inform on catalytic efficiency.[13,20] This parameter is most often tuned/modified by primary sphere considerations (e.g. ligand donor properties).[21] Given the accessibility of Cu–H units containing secondary sphere boranes, we examined the influence of the appended borane on subsequent Cu–H hydricity. In contrast to hydricity determination of Group 8-10 metal hydrides,[20a,22] there are comparatively few studies with copper hydrides.[9a,23] Thus, we determined the hydricity of both states of copper hydrides (monomer/dimer) using DFT with an approach previously described,[22] using $[Pt(dmpp)_2]^{2+}$ as the reference hydride acceptor (ΔG_{H^-} = 50.7

This article is protected by copyright. All rights reserved

Author Manuscript

kcal/mol).[24] To accurately model the solution behavior,[9a] we considered two cases to calculate the effective hydricity (total free energy of the reaction, see SI): 1) the binding of MeCN to Cu after hydride transfer, forming (L)Cu(NCMe) and, 2) binding of another Cu-H unit to form a bridged copper hydride $(L)_2Cu(\mu\text{-}H)$. [25] We validated this approach using simplified models of multinuclear copper hydride complexes reported by Appel[9a] and Buss,[23] and found a reasonable agreement with experimentally determined results (**Figure S50**). We extended our investigation to evaluate the hydricity of previously reported borane-capped cuprous hydrides (**Figure 5a**). Copper hydrides capped with either BH_3 or $B(C_6F_5)_3$ exhibit weak hydricity (**S2**: 73.8 kcal/mol and **S3**: 71.5 kcal/mol), consistent with a requirement for base and high temperature to react with CO_2. In contrast to these values, we found that the dimer, $[\mathbf{9}]_2$ is more hydridic (53.8 kcal/mol), and importantly, $\mathbf{9}^{mono}$ and $[\mathbf{9}]_2^{\mu\text{-}H}$ are *extremely* hydridic (24.9 and 33.2 kcal/mol, respectively).[26] We also considered a situation that forms an appended borohydride via Cu–H dissociation from $\mathbf{9}^{mono}$; however, we found that dissociation (concomitant with MeCN, THF, and benzene binding) was thermodynamically unfavorable (9.3, 5.7, 19.4 kcal/mol, respectively; **Figure S58**). One key finding is that the hydricity value of $\mathbf{9}^{mono}$, which is close to the hydricity values of unmasked monomeric Cu–H,[27] is not solely derived from Lewis acidity of the borane: an untethered variant, (^{Et}cAAC)CuH(EtBBN) (**S5**), has hydricity values in between the monomer and dimer (38.0 kcal/mol).

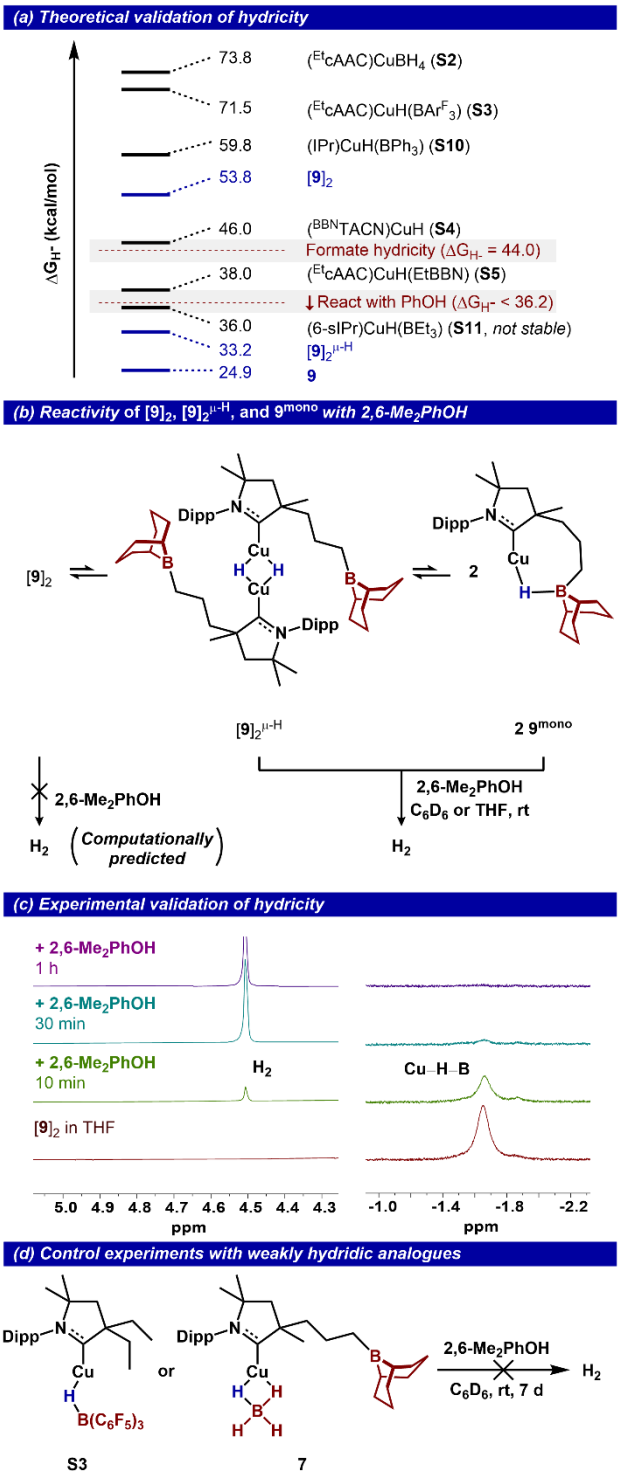


Figure 5. (a) Calculated hydricity of masked cuprous hydride (Gaussian 16 at *d3*-B3LYP/def2svp for Cu, 6-31+g(d,p) for B, C, N, H/CPCM(MeCN) level), (b) reactivity of $[\mathbf{9}]_2$ with 2,6-Me_2PhOH and their calculated hydricity, (c) its ^{1}H-NMR reaction monitoring, and (d) reactivity of **S3** and **7** with 2,6-Me_2PhOH.

To support the computational measurements, we experimentally estimated the hydricity by performing reactions with Brønsted acids with known pK_a values, a previously validated method.[20a,23] PhOH serves as a hydricity benchmark because it selectively reacts with metal hydrides possessing hydricities below 36.2 kcal/mol in MeCN (**Figure 5a**). Following deprotonation, the resulting OPh^- can coordinate to Cu, and this follow-up reaction can impact the overall free energy of the

This article is protected by copyright. All rights reserved

Author Manuscript

hydride transfer reaction. To limit this follow-up reaction and provide a more accurate assessment of hydricity, we employed sterically hindered PhOH derivatives (2,6-dimethylphenol (2,6-Me_2PhOH)). This derivative was previously used by Buss[23] to characterize a strongly hydridic Cu_3H_3 cluster (**S7**, ΔG_{H^-} = 26.6 kcal/mol).[28] Our calculated results suggest that $[\mathbf{9}]_2$ (ΔG_{H^-} = 53.8 kcal/mol) should *not* react with 2,6-Me_2PhOH. However, if an equilibrium of $[\mathbf{9}]_2$ with $\mathbf{9}^{mono}$ and $[\mathbf{9}]_2^{\mu\text{-}H}$ exists, the latter compounds would be anticipated to react with 2,6-Me_2PhOH to form H_2 due to their increased hydricity (**Figure 5b**).

Introduction of 1.5 equiv of 2,6-Me_2PhOH to a solution of $[\mathbf{9}]_2$ eliminated the Cu–H resonance within 1 h, and afforded H_2, as assessed by ^{1}H-NMR spectroscopy (in THF, **Figure 5c**; in C_6D_6, **Figure S33**). We also found that the more sterically hindered 2,4,6-tri-tert-butylphenol reacts with $[\mathbf{9}]_2$, albeit more slowly to produce H_2 (**Figure S34**). These results contrast with a parallel experiment using the structurally relevant but less hydridic (^{Et}cAAC)CuH(B(C_6F_5)$_3$) (**S3**) and **7**: we did not observe any reaction with 2,6-Me_2PhOH even after 7 d at room temperature (**Figure 5d**, **S35** and **S36**). Overall, these results demonstrate a clear deviation from anticipated reactivity from $[\mathbf{9}]_2$ and implicate an accessible equilibrium of $[\mathbf{9}]_2$ with $\mathbf{9}^{mono}$ and $[\mathbf{9}]_2^{\mu\text{-}H}$, compounds exhibiting very high hydricity.

To clarify the reasons governing the hydricity differences between $\mathbf{9}^{mono}$, $[\mathbf{9}]_2$ as well as other masked cuprous hydrides, we examined the structural and electronic properties of the Cu–H–B unit. These species can be formulated as either copper-coordinated borohydrides or borane-capped copper hydrides, and their location along this continuum may be informed by a Wiberg bond index (WBI) analysis.[12d] In contrast to $\mathbf{9}^{free}$, which exhibits a WBI for Cu–H of 0.76, $[\mathbf{9}]_2$ has a significantly lower value (0.18), indicating higher copper-borohydride character. $\mathbf{9}^{mono}$ and **S5** exhibit a slight increase in copper hydride character, with the WBI of 0.23 for both, consistent with their enhanced hydricity. The hydricity enhancement was augmented by analyses of their HOMO energies. The HOMO of $\mathbf{9}^{free}$ is heavily localized on the Cu–H bond and is -5.123 eV. The analogous orbital for $\mathbf{9}^{mono}$, $[\mathbf{9}]_2$, and **S5** is mixed across the Cu–H–B and lower in energy (-5.895 eV for $\mathbf{9}^{mono}$, -5.982, -6.006 eV for $[\mathbf{9}]_2$, and -6.150 eV for **S5**), attributable to stabilization of Cu–H by the Lewis acidic borane. These results, illustrating similar Cu–H–B bond energies, contrast with their notably different solution hydricities and suggest that additional factors are needed to describe the observed reactivity differences. Given that $\mathbf{9}^{mono}$ exhibits a more distorted angle between the $C^{carbene}$–Cu–(H–B centroid) than **S5** (150.6 º for $\mathbf{9}^{mono}$, 179.4 º for **S5**), we attribute this difference to a ring strain effect of $\mathbf{9}^{mono}$. We propose that release of this ring strain after hydride transfer provides additional thermodynamic stabilization, ultimately translating into higher hydricity.[29], [30]

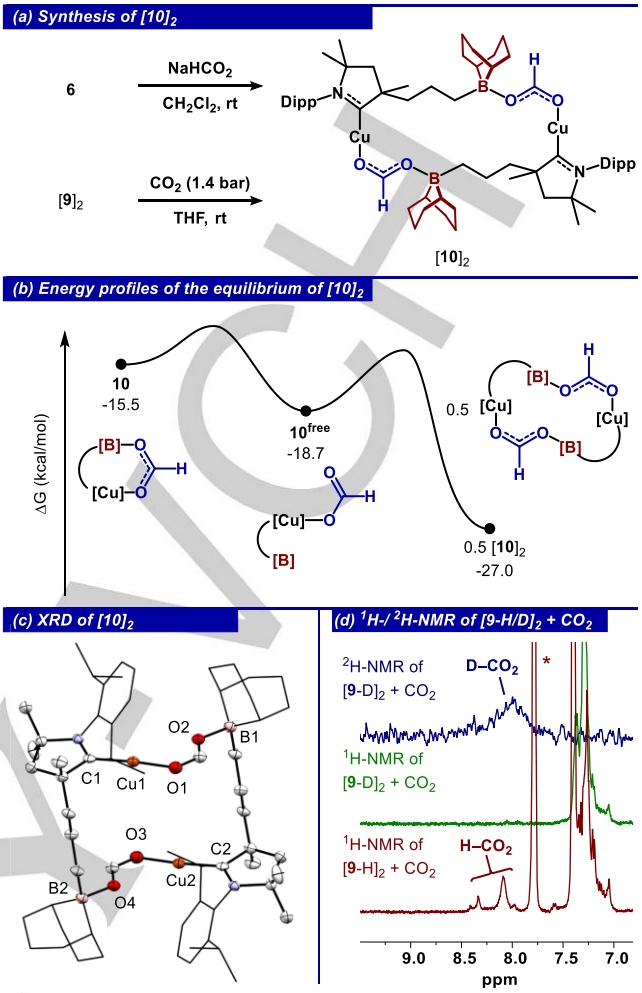
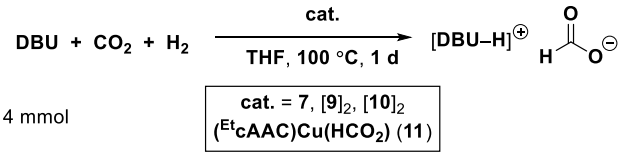


Figure 6. (a) Synthesis of $[\mathbf{10}]_2$, (b) energy profiles of the equilibrium of **9** (Gibbs free energies were calculated by Gaussian 16 at *d3*-B3LYP/def2svp for Cu, 6-31+g(d,p) for B, C, N, O, H/CPCM(THF) level), (c) solid state structure of $[\mathbf{10}]_2$, and (d) ^{1}H-/^{2}H-NMR of $[\mathbf{9}$-H/D$]_2$ with CO_2 in THF (* Naphthalene internal standard).

One important application of highly hydridic metal hydrides is their ability to reduce small molecule substrates, such as CO_2. Previously reported borane-masked cuprous hydrides required a long reaction time (> 6 h)[12d] or high temperatures (> 80 ºC)[11a] for CO_2 reactivity. In contrast to these forcing conditions, we found that $[\mathbf{9}]_2$ reacts *immediately* with 1.4 bar of CO_2 at room temperature, affording copper formate **10** (**Figure 6a**). Repeating this reaction sequence using deuterium labeled $[\mathbf{9}$-D$]_2$ provided further support of the hydride/deuteride delivery to CO_2. Analysis of the ^{2}H-NMR spectrum indicated that the Cu–D resonance of $[\mathbf{9}$-D$]_2$ (-1.65 ppm) converted into a new resonance at 7.98 ppm, which we assign as the Cu–DCO_2 resonance of **10**-D (**Figure 6d**). To facilitate characterization, we prepared **10** through an independent synthesis between **6** and $NaHCO_2$ in CH_2Cl_2. Similar to $[\mathbf{9}]_2$, the solid-state structure of **10** exhibited a dimeric structure $[\mathbf{10}]_2$ (**Figure 6c**), where a borane Lewis acid from an adjacent molecule interacts with the copper formate (Cu1–O1 = 1.872(2) Å, O2–B2 = 1.625(2) Å). DFT studies confirmed that the dimer was the most stable structure (**Figure 6b**), but unlike **9**, the intramolecular interaction between the formate and borane was not thermodynamically favored (+2.8 kcal/mol).

Author Manuscript

This article is protected by copyright. All rights reserved



Entry	cat. (mol% of [Cu])	Pressure (CO_2:H_2, bar)	Additive (mol%)	TON
1	[**10**]$_2$ (0.1)	16:48	-	241
2	[**10**]$_2$ (0.001)	16:48	-	375
3	[**10**]$_2$ (0.0001)	16:48	-	738
4	**7** (0.1)	16:48	-	215
5	[**9**]$_2$ (0.1)	16:48	-	140
6	[**10**]$_2$ (0.1)	8:24	-	77
7	[**10**]$_2$ (0.1)	8:24	**B(C_6F_5)$_3$** (0.1)	77
8	[**10**]$_2$ (0.1)	8:24	**B(C_6F_5)$_3$** (0.2)	76
9	**11** (0.1)	16:48	-	75
10	**11** (0.1)	16:48	**OctBBN** (0.1)	89
11	-	16:48	**OctBBN** (0.1)	6

Figure 7. (^{R}cAAC)Cu(HCO_2)-catalyzed CO_2 hydrogenation using H_2 (R = BBN and Et).

Our results showing rapid reactions between [**9**]$_2$ and CO_2 suggest that, if [**9**]$_2$ can be generated from H_2, it may be a competent catalyst for CO_2 hydrogenation. We examined the feasibility of this reaction sequence using [**10**]$_2$, which we anticipated should be an on-cycle catalytic intermediate. Addition of 1.0 equiv. DBU base to 0.05 mol% of [**10**]$_2$ (0.1 mol% of [Cu]) in THF under CO_2 and H_2 atmosphere (8 bar and 24 bar, respectively) at 100 ºC afforded [DBUH][HCO_2] with a turnover number (TON) of 77 (**Figure 7**, entry 6). Subsequently, we optimized the pressure, temperature, and catalyst loading (**Table S1**). Base optimization illustrated two key points to consider for an active hydrogenation catalyst containing an appended borane: 1) sufficient basicity to heterolyze H_2, and 2) appropriate steric/electronic match to prevent irreversible binding to the BBN Lewis acid at the reaction temperature. We found that DBU provided an appropriate balance of these two parameters (**Table S2**). However, in analogy to previous examples,[9a, 11a] we propose that dissociation of base (DBU) from Cu and borane center for H_2 activation requires thermal activation. Thus in contrast to stoichiometric CO_2 reactivity of [**9**]$_2$ at room temperature, catalytic reactions necessitate elevated reaction temperatures for catalytic CO_2 hydrogenation. Final optimized conditions indicate a TON of 241 to 738 with a catalyst loading of 0.1 to 0.0001 mol% (entries 1-3). Complexes **7** and [**9**]$_2$ were also active (TON = 215 and 140, respectively), with the latter supporting its role as a potential intermediate in the catalytic cycle (entries 4 and 5).

To provide a direct comparison with Bertrand's report using (cAAC)Cu and B(C_6F_5)$_3$,[11a] we evaluated reactions that included 1-2 equiv. B(C_6F_5)$_3$. We found that these modifications did not change the turnover number (TON) (entries 6-8), suggesting that the tethered BBN in the cAAC ligand outperforms an exogenous *stronger* borane in catalytic reactions. Similarly, a control experiment using 0.1 mol% of (^{Et}cAAC)CuHCO_2 (**11**) and 0.1 mol% of octyl BBN (octBBN; similar Lewis acidity to the tethered BBN group) (entries 9-11) did not improve the TON. These results underscore the feasibility of using weaker strength tethered secondary coordination sphere acids to outcompete stronger exogenous acids and improve the catalytic efficiency in CO_2 hydrogenation.

In summary, we have shown that BBN-tethered cAAC complexes can be prepared through late stage hydroboration. Although the appended BBN group serves to stabilize a dimeric cuprous hydride ([**9**]$_2$), equilibria with monomeric forms are feasible. Using computational hydricity determinations, we found that although [**9**]$_2$ is only moderately hydridic, the corresponding monomer is extremely hydridic, a result attributed to relief of ring strain after hydride transfer. We capitalized on the accessible solution hydricity for rapid reactions with CO_2 and phenol at room temperature. These stoichiometric studies were extended to catalytic efforts and we found that an intramolecular BBN group provides significant improvements in catalytic efficiency for CO_2 hydrogenation. Based on our results illustrating the impact of hydricity on ring strain of the resulting Cu–H–borane adduct, we anticipate that modifying the tether length would provide a unique strategy to tune hydricity independent of metal-based electronics, and these studies are ongoing in our group.

Acknowledgements

This work was supported by the NSF under award 2154678. N.K.S. is a Camille Dreyfus Teacher-Scholar. We thank Dr. Fengrui Qu for SCXRD data collection, Andrew Beamer and Prof. Joshua Buss for GC-FID measurement and discussions, Luis Garcia-Herrera and Prof. Charles McCrory for GC-TCD measurement.

Keywords: secondary sphere, Lewis acid, copper hydride, hydricity, CO_2 hydrogenation

[1] (a) C. Deutsch; N. Krause. *Chem. Rev.* **2008**, *108*, 2916-2927; (b) R. Y. Liu; S. L. Buchwald. *Acc. Chem. Res.* **2020**, *53*, 1229-1243

[2] (a) S. A. Bezman; M. R. Churchill; J. A. Osborn; J. Wormald. *J. Am. Chem. Soc.* **1971**, *93*, 2063-2065; (b) W. S. Mahoney; D. M. Brestensky; J. M. Stryker. *J. Am. Chem. Soc.* **1988**, *110*, 291-293; (c) J. F. Daeuble; J. M. Stryker. *e-EROS Encycl. Reagents Org. Synth.*, DOI: 10.1002/047084289X.rh047084011m

[3] (a) Y. Yang; S.-L. Shi; D. Niu; P. Liu; S. L. Buchwald. *Science* **2015**, *349*, 62-66; (b) Y. Xi; J. F. Hartwig. *J. Am. Chem. Soc.* **2017**, *139*, 12758-12772

[4] (a) N. P. Mankad; D. S. Laitar; J. P. Sadighi. *Organometallics* **2004**, *23*, 3369-3371; (b) G. D. Frey; B. Donnadieu; M. Soleilhavoup; G. Bertrand. *Chem. Asian. J.* **2011**, *6*, 402-405; (c) L. R. Collins; I. M. Riddlestone; M. F. Mahon; M. K. Whittlesey. *Chem. Eur. J.* **2015**, *21*, 14075-14084; (d) S. C. Schmid; R. Van Hoveln; J. W. Rigoli; J. M. Schomaker. *Organometallics* **2015**, *34*, 4164-4173; (e) A. J. Jordan; C. M. Wyss; J. Bacsa; J. P. Sadighi. *Organometallics* **2016**, *35*, 613-616; (f) T. G. Carroll; D. E. Ryan; J. D. Erickson; R. M. Bullock; B. L. Tran. *J. Am. Chem. Soc.* **2022**, *144*, 13865-13873

[5] (a) G. V. Goeden; K. G. Caulton. *J. Am. Chem. Soc.* **1981**, *103*, 7354-7355; (b) S. Zhang; H. Fallah; E. J. Gardner; S. Kundu; J. A. Bertke; T. R. Cundari; T. H. Warren. *Angew. Chem. Int. Ed.* **2016**, *55*, 9927-9931; (c) A. N. Desnoyer; A. Nicolay; M. S. Ziegler; N. A. Torquato; T. D. Tilley. *Angew. Chem. Int. Ed.* **2020**, *59*, 12769-12773; (d) A. Grasruck; G. Parla; L. Lou; J. Langer; C. Neiß; A. Herrera; S. Frieß; A. Görling; G. Schmid; R. Dorta. *Chem. Commun.* **2023**, *59*, 13879-13882

[6] The most common strategy to obtain copper hydrides is to use borohydrides, hydroboranes, and hydrosilanes with anionic activators.

[7] (a) W. S. Mahoney; J. M. Stryker. *J. Am. Chem. Soc.* **1989**, *111*, 8818-8823; (b) J.-X. Chen; J. F. Daeuble; J. M. Stryker. *Tetrahedron* **2000**, *56*, 2789-2798; (c) H. Shimizu; D. Igarashi; W. Kuriyama; Y. Yusa; N. Sayo; T. Saito. *Org. Lett.* **2007**, *9*, 1655-1657; (d) K. Junge; B. Wendt; D. Addis; S. Zhou; S. Das; S. Fleischer; M. Beller. *Chem. Eur. J.* **2011**, *17*, 101-105; (e) F. Pape; N. O. Thiel; J. F. Teichert. *Chem. Eur. J.* **2015**, *21*, 15934-15938; (f) B. M. Zimmermann; T. T. Ngoc; D.-l. Tzaras; T. Kaicharla; J. F. Teichert. *J. Am. Chem. Soc.* **2021**, *143*, 16865-16873

[8] (a) T. H. Lemmen; K. Folting; J. C. Huffman; K. G. Caulton. *J. Am. Chem. Soc.* **1985**, *107*, 7774-7775; (b) E. Kounalis; M. Lutz; D. L. J. Broere. *Chem. Eur. J.* **2019**, *25*, 13280-13284; (c)

Author Manuscript

This article is protected by copyright. All rights reserved

D. A. Ekanayake; A. Chakraborty; J. A. Krause; H. Guan. *Inorg. Chem.* **2020**, *59*, 12817-12828

[9] (a) C. M. Zall; J. C. Linehan; A. M. Appel. *J. Am. Chem. Soc.* **2016**, *138*, 9968-9977; (b) A. Aloisi; É. Crochet; E. Nicolas; J.-C. Berthet; C. Lescot; P. Thuéry; T. Cantat. *Organometallics* **2021**, *40*, 2064-2069

[10] (a) D. W. Stephan; G. Erker. *Angew. Chem. Int. Ed.* **2010**, *49*, 46-76; (b) D. W. Stephan. *J. Am. Chem. Soc.* **2015**, *137*, 10018-10032; (c) A. J. M. Miller; J. A. Labinger; J. E. Bercaw. *J. Am. Chem. Soc.* **2008**, *130*, 11874-11875; (d) A. J. M. Miller; J. A. Labinger; J. E. Bercaw. *J. Am. Chem. Soc.* **2010**, *132*, 3301-3303; (e) A. M. Chapman; M. F. Haddow; D. F. Wass. *J. Am. Chem. Soc.* **2011**, *133*, 18463-18478; (f) A. J. M. Miller; J. A. Labinger; J. E. Bercaw. *Organometallics* **2011**, *30*, 4308-4314; (g) Y. Jiang; O. Blacque; T. Fox; H. Berke. *J. Am. Chem. Soc.* **2013**, *135*, 7751-7760; (h) R. M. Bullock; G. M. Chambers. *Philosophical Transactions of the Royal Society A: Mathematical, Physical and Engineering Sciences* **2017**, *375*, 20170002

[11] (a) E. A. Romero; T. Zhao; R. Nakano; X. Hu; Y. Wu; R. Jazzar; G. Bertrand. *Nat. Catal.* **2018**, *1*, 743-747; (b) H. Luo; B. Zhu; X. Liu; X. Zhang; T. Zhao; X. Hu. *Mol. Catal.* **2023**, *546*, 113198

[12] (a) X. Hu; M. Soleilhavoup; M. Melaimi; J. Chu; G. Bertrand. *Angew. Chem. Int. Ed.* **2015**, *54*, 6008-6011; (b) L. R. Collins; N. A. Rajabi; S. A. Macgregor; M. F. Mahon; M. K. Whittlesey. *Angew. Chem. Int. Ed.* **2016**, *55*, 15539-15543; (c) F. Ritter; D. Mukherjee; T. P. Spaniol; A. Hoffmann; J. Okuda. *Angew. Chem. Int. Ed.* **2019**, *58*, 1818-1822; (d) E. E. Norwine; J. J. Kiernicki; M. Zeller; N. K. Szymczak. *J. Am. Chem. Soc.* **2022**, *144*, 15038-15046

[13] M. S. Jeletic; E. B. Hulley; M. L. Helm; M. T. Mock; A. M. Appel; E. S. Wiedner; J. C. Linehan. *ACS Catal.* **2017**, *7*, 6008-6017

[14] (a) J. A. Zurakowski; B. J. H. Austen; M. W. Drover. *Trends Chem.* **2022**, *4*, 331-346; (b) J. J. Kiernicki; M. Zeller; N. K. Szymczak. *J. Am. Chem. Soc.* **2017**, *139*, 18194-18197; (c) H. L. Li; Y. Kuninobu; M. Kanai. *Angew. Chem. Int. Ed.* **2017**, *56*, 1495-1499; (d) J. J. Kiernicki; E. E. Norwine; M. Zeller; N. K. Szymczak. *Chem. Commun.* **2019**, *55*, 11896-11899; (e) J. J. Kiernicki; J. P. Shanahan; M. Zeller; N. K. Szymczak. *Chem. Sci.* **2019**, *10*, 5539-5545; (f) J. J. Kiernicki; M. Zeller; N. K. Szymczak. *Inorg. Chem.* **2019**, *58*, 1147-1154; (g) L. Yang; N. Uemura; Y. Nakao. *J. Am. Chem. Soc.* **2019**, *141*, 7972-7979; (h) J. J. Kiernicki; E. E. Norwine; M. A. Lovasz; M. Zeller; N. K. Szymczak. *Chem. Commun.* **2020**, *56*, 13105-13108; (i) J. J. Kiernicki; M. Zeller; N. K. Szymczak. *Inorg. Chem.* **2020**, *59*, 9279-9286; (j) J. J. Kiernicki; M. Zeller; N. K. Szymczak. *Organometallics* **2021**, *40*, 2658-2665; (k) J. A. Zurakowski; B. J. H. Austen; M. C. Dufour; M. Bhattacharyya; D. M. Spasyuk; M. W. Drover. *Dalton Trans.* **2021**, *50*, 12440-12447; (l) J. A. Zurakowski; B. J. H. Austen; M. C. Dufour; D. M. Spasyuk; D. J. Nelson; M. W. Drover. *Chem. Eur. J.* **2021**, *27*, 16021-16027; (m) J. A. Zurakowski; M. Bhattacharyya; D. M. Spasyuk; M. W. Drover. *Inorg. Chem.* **2021**, *60*, 37-41; (n) B. Wang; C. S. G. Seo; C. Zhang; J. Chu; N. K. Szymczak. *J. Am. Chem. Soc.* **2022**, *144*, 15793-15802; (o) M. L. Clapson; H. Sharma; J. A. Zurakowski; M. W. Drover. *Chem. Eur. J.* **2023**, *29*, e202203763

[15] M. Toure; O. Chuzel; J.-L. Parrain. *Dalton Trans.* **2015**, *44*, 7139-7143

[16] J. Chu; D. Munz; R. Jazzar; M. Melaimi; G. Bertrand. *J. Am. Chem. Soc.* **2016**, *138*, 7884-7887

[17] (a) J. Monot; L. Fensterbank; M. Malacria; E. Lacôte; S. J. Geib; D. P. Curran. *Beilstein J. Org. Chem.* **2010**, *6*, 709-712; (b) R. Kinjo; B. Donnadieu; M. A. Celik; G. Frenking; G. Bertrand. *Science* **2011**, *333*, 610-613; (c) D. A. Ruiz; G. Ung; M. Melaimi; G. Bertrand. *Angew. Chem. Int. Ed.* **2013**, *52*, 7590-7592; (d) D. Auerhammer; M. Arrowsmith; H. Braunschweig; R. D. Dewhurst; J. O. C. Jiménez-Halla; T. Kupfer. *Chem. Sci.* **2017**, *8*, 7066-7071

[18] **8** reveals a slightly shorter B1–C1 bond length (1.597(3) Å) than that in the reported RBH_2-cAAC adducts (R = neopentyl, 1.604(2) Å; R = mesityl, 1.611(3) Å),[17d] likely due to its stronger intramolecular interaction.

[19] A. D. Bage; K. Nicholson; T. A. Hunt; T. Langer; S. P. Thomas. *Synthesis* **2022**, *55*, 62-74

[20] (a) E. S. Wiedner; M. B. Chambers; C. L. Pitman; R. M. Bullock; A. J. M. Miller; A. M. Appel. *Chem. Rev.* **2016**, *116*, 8655-8692; (b) K. M. Waldie; A. L. Ostericher; M. H. Reineke; A. F. Sasayama; C. P. Kubiak. *ACS Catal.* **2018**, *8*, 1313-1324

[21] (a) M. R. Espinosa; M. Z. Ertem; M. Barakat; Q. J. Bruch; A. P. Deziel; M. R. Elsby; F. Hasanayn; N. Hazari; A. J. M. Miller; M. V. Pecoraro; A. M. Smith; N. E. Smith. *J. Am. Chem. Soc.* **2022**, *144*, 17939-17954; (b) K. Schlenker; L. K. Casselman; R. T. VanderLinden; C. T. Saouma. *Catal. Sci. Technol.* **2023**, *13*, 1358-1368

[22] X.-J. Qi; Y. Fu; L. Liu; Q.-X. Guo. *Organometallics* **2007**, *26*, 4197-4203

[23] A. W. Beamer; J. A. Buss. *J. Am. Chem. Soc.* **2023**, *145*, 12911-12919

[24] C. J. Curtis; A. Miedaner; W. W. Ellis; D. L. DuBois. *J. Am. Chem. Soc.* **2002**, *124*, 1918-1925

[25] For hydricity calculations, we considered the solvation effect by MeCN to be able to directly compare our results with previous reports.

[26] E. A. Patrick; M. E. Bowden; J. D. Erickson; R. M. Bullock; B. L. Tran. *Angew. Chem. Int. Ed.* **2023**, *62*, e202304648

[27] Monomeric (^{Et}cAAC)CuH and **9**^{free} exhibit hydricity values of 24.1 and 24.0 kcal/mol, respectively.

[28] The copper bromide analog of **S7** features a similar buried volume (V_{bur}) to **5** (**Figure S48**).

[29] J. W. Raebiger; A. Miedaner; C. J. Curtis; S. M. Miller; O. P. Anderson; D. L. DuBois. *J. Am. Chem. Soc.* **2004**, *126*, 5502-5514

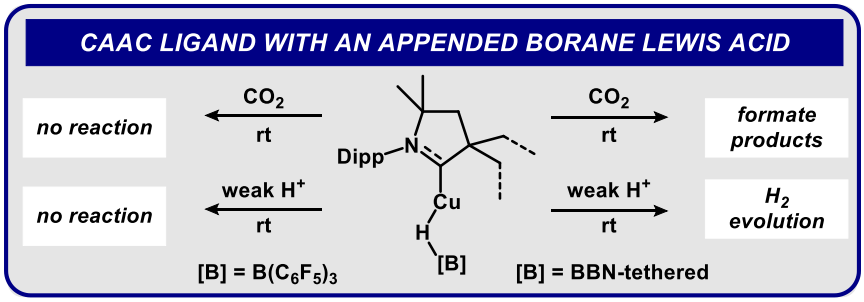
[30] To comprehend the three-center two-electron (3c2e) bonding interaction of Cu–H–B, we examined how the copper hydride character changed with the bonding angle (**Figure S51**). As the bond angle of Cu–H–B decreased, the WBI of Cu–H decreased, and the WBI of B–H increased. Furthermore, the H contribution to the 3c2e interaction increased while the B contribution decreased. The decrease in Cu contribution was relatively less pronounced compared to that of B.

[31] Deposition Number(s): 2351021 (for [**2**]BF_4), 2351022 (for **3**), 2351023 (for **5**), 2351024 (for **7**), 2351025 (for **8**), 2351026 (for [**10**]$_2$), 2351027 (for **S13**) contain the supplementary crystallographic data for this paper. These data are provided free of charge by the joint Cambridge Crystallographic Data Centre and Fachinformationszentrum Karlsruhe Access Structures service.

Author Manuscript

This article is protected by copyright. All rights reserved

Entry for the Table of Contents



A Lewis acidic borane was introduced into the secondary coordination sphere of cyclic (alkyl)(amino)carbene (cAAC) copper complexes, including a cuprous hydride. In contrast to non-tethered borane capped copper hydrides, the borane-tethered variant exhibits strong hydricity, attributed to relief of ring-strain, and improved catalytic efficiency.

Institute and/or researcher Twitter usernames: @SzymczakLab, @HSong_chem

WILEY-VCH

Author Manuscript

This article is protected by copyright. All rights reserved